Hole-drift velocity in natural diamond

L. Reggiani, S. Bosi, C. Canali, and F. Nava
Gruppo Nazionale di Struttura della Materia, Istituto di Fisica, Università di Modena, Via Campi, 213/A, 41100 Modena, Italy

S. F. Kozlov
P. N. Lebedev Physical Institute of the Union of Soviet Socialist Republic Academy of Science, Moscow V-372, Leninsky pr 53, Union of Soviet Socialist Republic

(Received 4 April 1980)

The drift velocity of holes in natural diamond is analyzed for a wide range of temperatures $85 \leq T \leq 700$ K and fields $10^2 < E < 6 \times 10^4$ V/cm applied parallel to ⟨100⟩ and ⟨110⟩ crystallographic directions. Experiments are carried out with the time-of-flight technique, and theory uses a Monte Carlo method. The microscopic interpretation is based on a two-spherical and parabolic band model and considers lattice scattering only. Values $m_h = 1.1\ m_o$ and $m_l = 0.3\ m_o$ for heavy- and light-hole effective masses are found.

I. INTRODUCTION

This work, the fifth of a series of papers devoted to the study of carrier drift velocity in elemental semiconductors of group four,[1-4] presents an experimental and theoretical investigation of the drift velocity of holes in natural diamond as a function of temperature and electric field applied parallel to different crystallographic directions.[5]

Few data exist in the literature on transport properties of holes.[8] Hall mobility has been reported by different authors[9-13] and among them the most recent, Refs. 12 and 13, summarize well the behavior of the Hall mobility in the $110 < T < 1000$ K temperature range. In Ref. 13 data of Hall mobility as a function of electric field strength at 120 K were also presented.

Concerning the microscopic interpretation, the values of the effective masses of holes are still an open problem. In fact, the values deduced from cyclotron resonance experiments of Rauch[14] were found to disagree both with values obtained from transport experiments[15] and band-structure calculations.[16,17] As an example, under $\epsilon/\Delta \gg 1$ conditions (ϵ being the hole energy and $\Delta = 0.006$ eV the spin-orbit energy) the density-of-states effective mass for heavy and light holes calculated as in Ref. 18 are $m_h = 2.30 m_0$, $m_l = 2.08 m_0$ (m_0 being the free electron mass) with the Rauch parameters[14] and $m_h = 0.40 m_0$, $m_l = 0.28 m_0$ with the Lawaetz parameters.[17] Furthermore, very little is known on the deformation potential parameters describing lattice scattering interaction.

The aim of this paper is to present a systematic set of experimental data of the hole-drift velocity and, from a theoretical interpretation, to suggest reliable values for the hole effective masses and deformation potentials. Measurements of the drift velocity are performed in the temperature range $85 \leq T \leq 700$ K and for electric fields between 10^2 and 6×10^4 V/cm applied parallel to the crystallographic directions ⟨100⟩ and ⟨110⟩. Furthermore, experimental results evidence an anisotropic effect of the hole-drift velocity along ⟨110⟩ and ⟨100⟩ crystallographic directions. The theoretical analysis makes use of a spherical and parabolic two-band model together with a Monte Carlo technique in solving the Boltzmann equation. The two effective masses and the two deformation potential constants for acoustic and nonpolar optical scattering will be considered adjustable parameters. The comparison between theory and experiments will suggest a choice for these parameters. Section II describes the experimental technique and reports the data; the theoretical approach together with the discussion of the results is given in Sec. III.

II. SAMPLES, EXPERIMENTAL TECHNIQUE, AND RESULTS

The natural diamond crystals used here come from the Yakutia (Siberia, U. S. S. R.) deposit and are selected by photoconductivity and absorption coefficient measurements to ensure a nitrogen concentration not exceeding 10^{19} cm^{-3} (nitrogen acts as deep donor[19]) and a bulk lifetime not less than 5×10^{-9} sec. Samples with a thickness ranging from 60 to 420 μm and a useful area of about 10 mm^2 are obtained from different crystals; x-ray diffraction analysis shows that the surfaces of the samples are perpendicular to the crystallographic axes ⟨100⟩ ± 1° and ⟨110⟩ ± 15°. To measure transport properties, contacts are made through an evaporation of gold or aluminum on diamond plates mechanically and chemically polished. As described in more detail elsewhere,[20] a few samples are provided with boron-implanted contacts. Those should ensure hole injection, thus avoiding polarization effects in time-of-flight technique; in the measurements no difference has been detected

TABLE I. Characteristics of the samples used in drift velocity measurements.

Thickness (μm)	Crystal axis	Mean free drift time (10^{-9} sec)	Mobility at 300 K (cm^2/V sec)	Acceptor trap energy (eV)	Acceptor trap density (cm^{-3})
200	⟨100⟩	8	2080		
322	⟨100⟩	17	2140		
420	⟨100⟩	12	2100		
60	⟨110⟩	7	2150		
120	⟨110⟩	12	2110	0.6; 0.8	10^{12}–10^{13}
225	⟨110⟩	9	2080		
305	⟨110⟩	7	2100	0.6; 0.8	10^{12}–10^{13}
400	⟨110⟩	15	2050		

between different samples under pulsed applied voltage conditions. To better characterize the samples, measurements of space-charge-limited current and thermally stimulated current were performed on those with boron-implanted contacts.[21] Results have indicated the presence of two active traps at about 0.6 and 0.8 eV above the valence band, with densities ranging between 10^{12} and 10^{13} cm^{-3}. These traps should be responsible for the relatively short trapping times which have been observed both with nuclear[22] and time-of-flight techniques. The sample characteristics are reported in Table I.

In the present experiments, samples are fitted in between two boron-nitride pierced disks and included in a copper container. The boron-nitride disks guarantee a good thermal coupling and electric insulation between the sample and the copper container.

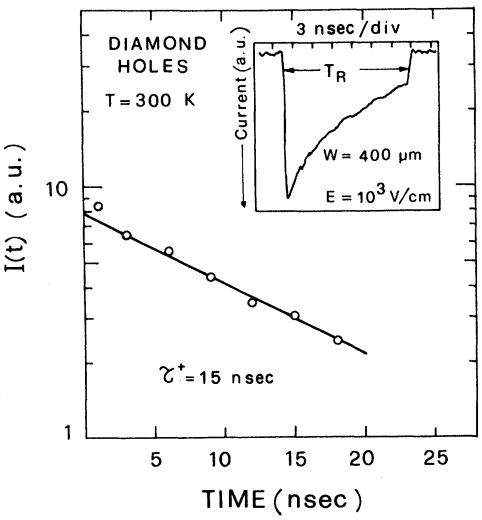

FIG. 1. Shape of the current pulse induced by the drift of holes and plot of the exponential decay on a semilog scale at room temperature in a 400-μm thick and ⟨110⟩ oriented sample with $E = 10^3$ V/cm.

The drift velocity of holes and therefore their mobility are obtained with the time-of-flight technique[23] by measuring the transit time which the holes created in proximity of the positive electrode take to reach the negative one, by crossing the crystal. The measurement of the transit time T_R is made as function of electric field and temperature by employing a pulsed electron accelerator[24] as source of the ionizing radiation.

In the case of trapping with negligible detrapping, the hole mean free drift time, τ_h^+, has been measured[23,25,26] from the sag on the top of the current pulse and plotted in a semilog scale. Figure 1 shows the current signal induced by holes crossing the sample as obtained with the pulsed electron accelerator. It refers to a 400-μm thick sample with an electric field $E = 10^3$ V/cm at $T = 300$ K. The exponential decay of the current pulse enables measurement of τ_h^+ to be carried out easily. The values of τ_h^+ which are measured in the samples used in the present work are reported in Table I. In the examined range of electric fields, the hole mean free drift time τ_h^+ does not change with E, and increases slightly by increasing the temperature, as shown in Fig. 2. This suggests that only small variations occur in the concentration of the active traps or in their capture cross section and enables measurements to be performed in a wide range of temperature.

A discussion of the experimental sources of errors affecting the drift-velocity measurements as a function of electric field and temperature is reported in Ref. 1. The total error in the present drift-velocity measurements should be within ± 5% at low electric fields and ± 3% at high electric fields. The maximum error in the electric field determination is estimated to be less than ± 3%. Finally, the error in the temperature is less than ± 2 K.

The hole-drift velocity is reported as a function of electric field applied parallel to the ⟨110⟩ crystallographic direction at the different temperatures

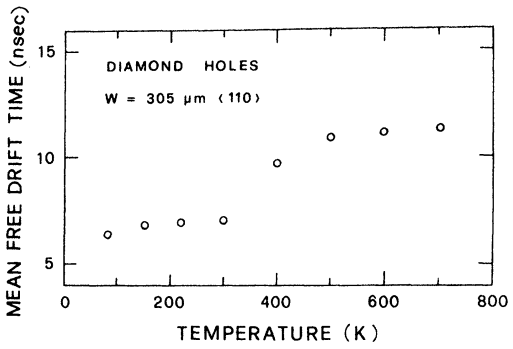

FIG. 2. Hole mean free drift time as a function of temperature in a 305-μm thick ⟨110⟩ oriented sample.

indicated in Fig. 3 (filled circles represent there an average value of the experimental data). In the limited temperature range $85 \leq T \leq 300$ K, measurements with the electric field applied parallel to the ⟨100⟩ crystallographic direction are performed. Results show an appreciable difference from those obtained with $\vec{E} \parallel \langle 110 \rangle$, particularly at low temperatures. Therefore, to better display this anisotropic effect, the drift velocities as a function of the electric field applied parallel to the ⟨100⟩ and ⟨110⟩ axes are reported in Fig. 4 at the temperatures indicated.

The drift mobility obtained from the ratio between drift velocity and electric field, v_d/E, at the lowest field strength is reported in Fig. 5 together with Hall mobility data reported in literature. Drift mobility results agree well with Hall mobility data at high temperatures ($T > 400$ K), while below 400 K present data exhibit a mobility higher by about 40%. This difference can be attributed to the greater perfection of the samples here used and/or to the difference between Hall and drift mobility. Let us note that in this latter case diamond behaves like silicon, for which a drift mobility higher than Hall mobility has been found under negligible impurity scattering.[27]

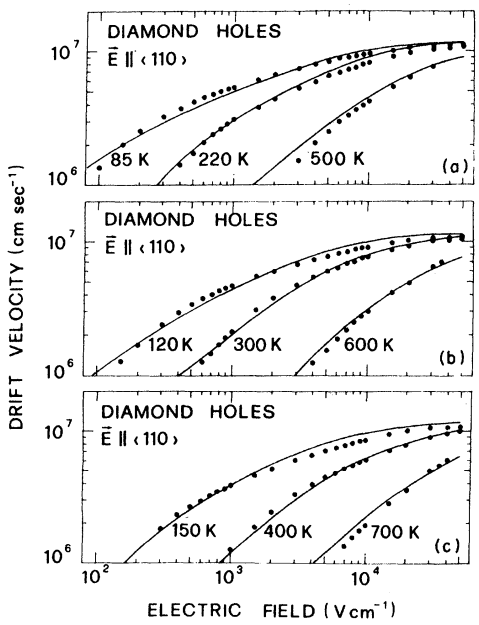

FIG. 3. Hole-drift velocity v_d as a function of electric field E applied parallel to ⟨110⟩ direction at the different temperatures indicated. Filled circles refer to experimental data, continuous lines indicate the theoretical results.

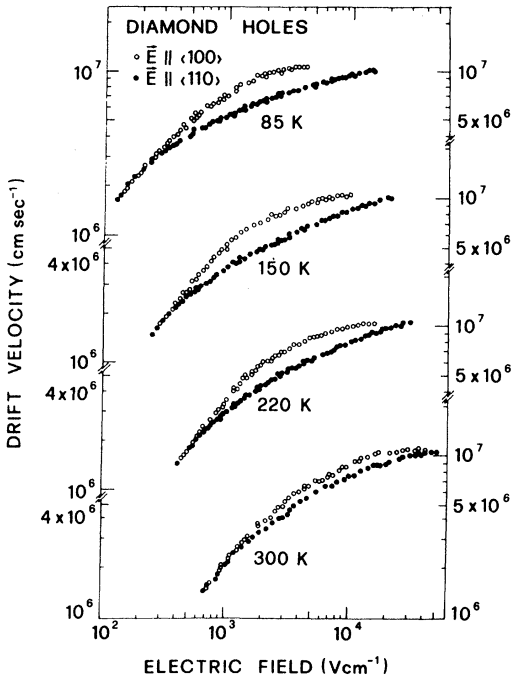

FIG. 4. Hole-drift velocity v_d as a function of electric field E at the different temperatures indicated. Open and filled circles refer to experimental data obtained with the field parallel to ⟨100⟩ and ⟨110⟩ directions, respectively. Continuous lines report the theoretical results.

The main features of the present experimental results can be summarized as follows:

(i) Drift mobility exhibits the typical $T^{-1.5}$ dependence at temperatures below 400 K, while above about 400 K the slope becomes steeper towards a $T^{-2.8}$ dependence.

(ii) At increasing field strength the drift velocity exhibits a sublinear dependence with field which is characteristic of covalent semiconductors.[28] Furthermore, for $T \leq 300$ K an anisotropic effect is observed with $v_{d100} \geq v_{d110}$. This anisotropic effect is found to increase by lowering the temperature,

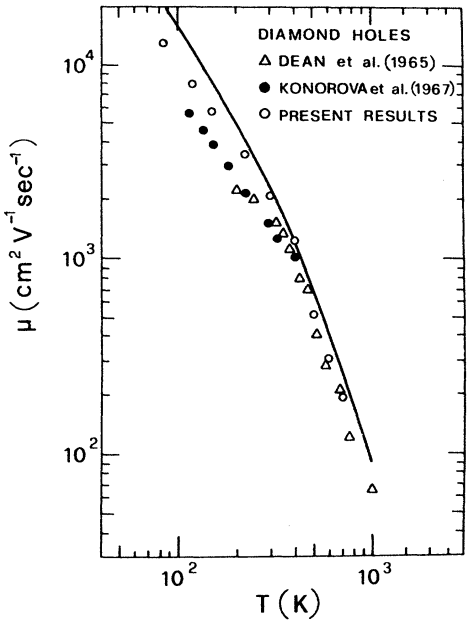

FIG. 5. Hole mobility as a function of temperature in natural diamond. Δ refers to Hall mobility data of Ref. (12); ● refers to Hall mobility data of Ref. (13); O refers to present results. The continuous curve refers to theoretical calculations.

its maximum effect, with a $(v_{d\,100}/v_{d\,110}-1)\simeq 40\%$, being observed at $T=85$ K for $E=2.5$ kV/cm.

(iii) For temperatures below about 300 K a saturated region of drift velocity is found at the highest applied fields ($Ep\simeq 5\times 10^4$ V/cm). From these results a value of the saturated drift velocity $v_s=1.1\pm 0.1\times 10^7$ cm/sec for all temperatures below about 300 K can be extrapolated. This saturation effect disappears at increasing temperatures.

III. THEORETICAL APPROACH

A. Microscopic model

The theoretical approach makes use of a two-band model, the heavy and light hole characterized by effective masses m_h and m_l, which is spherical and parabolic. Owing to the purity of the material and to the temperatures here investigated, only lattice scattering mechanisms have been considered. Accordingly, acoustic and nonpolar scattering mechanisms are accounted for. The former assumes a single constant for treating the acoustic coupling and includes overlap effects, acoustic energy dissipation, and the exact Bose-Einstein phonon distribution as reported in Ref. 29. The Boltzmann equation is solved through the Monte Carlo technique[3] and the estimated uncertainty in the computed values is at most 5%.

The similarities of the valence band of diamond with those of Si and Ge (Ref. 17) justify the present choice for the band model. In fact, at the temperatures and fields here considered, the asymptotic band shape, corresponding to the condition $\epsilon/\Delta\gg 1$, can be assumed. Under this condition, following Kane's results,[30] the three valence bands exhibit a parabolic behavior and are characterized by a warped shape of their equienergetic surfaces, which is more pronounced in the case of heavy holes. However, to avoid the main analytical difficulties encountered in including the rigorous energy dispersion relationship of Kane,[30] the third band is omitted and the warping is neglected. The omission of the third band, which is split off by spin-orbit interaction and whose effective mass takes the smallest value, is justified by its smallest density of states. Neglect of warping does not enable a quantitative interpretation of anisotropic effects to be carried out.

B. Fitting procedure

Since large discrepancies arise in literature concerning the values of the effective masses[7] and very little is known about the acoustic E_1^0 and optical $(D_tK)_{op}$ deformation potentials, in principle our theoretical approach has four adjustable parameters, that is, m_h, m_l, E_1^0, and $(D_tK)_{op}$. As will be reported below, the selective sensitivity of the drift velocity to different parameters in different regions of temperature and field strengths enables us to determine m_h, E_1^0, and $(D_tK)_{op}$, while as a working assumption $m_l=0.3m_0$ is taken.

The theoretical interpretation of the temperature dependence of mobility enables a combination of the hole effective masses and deformation potential parameters to be determined. As a guideline, the usual relaxation-time approximation for mobility can be used. Within this approximation the acoustic limited mobility μ_{ac} can be written as[31]

$$\mu_{ac}=\sigma T^{-3/2}, \tag{1}$$

$$\sigma=\frac{2^{5/2}\pi^{1/2}e\hbar^4\rho s^2}{3K_B^{3/2}}\,\frac{1+(m_h/m_l)^{1/2}}{E_1^{0\,2}m_l^{5/2}[1+(m_h/m_l)^{3/2}]^2}, \tag{2}$$

ρ being the crystal density, $s=\frac{1}{3}(2s_t+s_l)$ the average sound velocity, e the unit charge, $\hbar$ the Planck constant divided by 2π, and K_B the Boltzmann constant.

Since ρ and s are known independently (see Table II), for a given set of m_h and m_l the fitting of acoustic mobility in the temperature range below about 400 K enables us to determine a value of the acoustic deformation potential E_1^0 from Eq. (2).

For temperatures above about 400 K the devia-

TABLE II. Constants of diamond.

Lattice constant	$a_0 = 3.57 \times 10^{-8}$ cm	Ref. 33
Crystal density	$\rho = 3.51$ g cm^{-3}	Ref. 34
Longitudinal sound velocity	$s_l = 18.21 \times 10^5$ cm sec^{-1}	Ref. 35
Transverse sound velocity	$s_t = 12.30 \times 10^5$ cm sec^{-1}	Ref. 35
Optical phonon equivalent temp.	$\theta_{op} = 1938$ K	Ref. 8
Static dielectric constant	$\epsilon_0 = 5.7$	Ref. 12
Energy gap	$E_g = 5.49$ eV	Ref. 8
Spin orbit energy	$\Delta = 0.006$ eV	Ref. 8
Heavy-hole effective mass	$m_h = 1.1$	Ref. 7
Light-hole effective mass	$m_l = 0.3$	Ref. 7
Acoustic deformation potential	$E_1^0 = 5.5$ eV	Ref. 7
	$(D_t K)_{op} = 21 \times 10^8$ eV cm^{-1}	
Optical deformation potential [a]	$d_0 = 61.2$ eV	Ref. 7

[a] The two formalisms are related by $(D_t K)_{op} = (\frac{3}{2})^{1/2} d_0/a_0$.

tion from the $T^{-3/2}$ law of mobility is naturally interpreted by the onset of optical phonon scattering. This in turn will enable us to determine the value of the optical deformation potential parameter $(D_t K)_{op}$ for the same set of m_h and m_l.

For temperatures much lower than the equivalent optical phonon temperature θ_{op}, the theoretical interpretation of the drift velocity in the saturated region enables the determination of the heavy-hole effective mass to be carried out. As a guideline, the streaming motion approximation[32] is assumed. This approximation for a simple band model leads to the following results for the saturated drift velocity v_s and the mean energy $\langle \epsilon \rangle$:

$$v_s = \left(\frac{K_B \theta_{op}}{2 m_0} \right)^{1/2}, \tag{3}$$

$$\langle \epsilon \rangle = \tfrac{1}{3} K_B \theta_{op}. \tag{4}$$

The reliability of Eqs. (3) and (4) for the two-band model here used is questionable. However, Monte Carlo calculations lead to the two following conclusions in support of the above approximation:

(i) When m_0 is substituted for by m_h, Eq. (3) agrees within a few percent with the results of the Monte Carlo calculations.

(ii) Within its range of variability $0 < m_l < m_h$, the light-hole effective mass can increase the value of the saturated drift velocity by no more than about 10% with respect to the value calculated with the heavy-hole effective mass only.

Since θ_{op} is known independently, the fitting of the saturated drift velocity enables us to determine a value of the heavy-hole effective mass m_h from Eq. (3). To support the reliability of this fitting procedure, the starting point used for Monte Carlo calculations is briefly illustrated in the following. The fitting of the experimental $v_s = 1.1 \times 10^7$ cm/sec with Eq. (3) leads to $m_h = 1.21 m_0$. Using the set $m_h = 1.21 m_0$, $m_l = 0.3 m_0$, the fitting of the experimental $\alpha = 1.10 \times 10^7$ cm^2 K$^{3/2}$/(V sec) with Eq. (2) leads to $E_1^0 = 5.5$ eV. Further Monte Carlo calculations show that a 10% decrease of the initial m_h value enables the fitting of the high-field data to be improved. Accordingly, Table II reports the final set of the parameters used which are found to better interpret experiments in the whole range of fields and temperatures together with other parameters of interest for diamond.

C. Ohmic mobility

The theoretical values of mobility are obtained from the v_d/E ratio at field strengths low enough to satisfy within the computational uncertainty the thermal equilibrium condition $\langle \epsilon \rangle = \frac{3}{2} k_B T$. Figure 5 compares present theoretical results with experiments. The agreement is found to be satisfactory near room temperature, while at low and high temperatures theoretical results are slightly higher than experimental ones. Some dependence with field of the experimental data in the low temperature region and the approximations introduced in the theoretical model should justify this remaining discrepancy. Concerning the importance of different lattice scatterings, it is found that for temperature below about 400 K acoustic scattering only controls mobility, while above about 400 K the onset of optical scattering mechanism is responsible for the steeper dependence of the mobility versus temperature curve.

Figure 6 compares the theoretical results of the mobility versus temperature curve obtained with three different band models: the present one ($m_h = 1.1 m_0$, $m_l = 0.3 m_0$) and those of Rauch[14] ($m_h = 2.30 m_0$, $m_l = 2.08 m_0$) and Lawaetz[17] ($m_h = 0.40 m_0$, $m_l = 0.28 m_0$) which, within the models achievable from literature,[14,16,17] can be considered as ex-

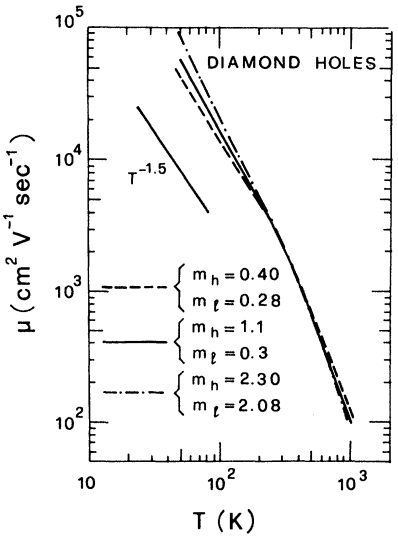

FIG. 6. Theoretical hole mobility as a function of temperature. Dot-dashed curve refers to Rauch (Ref. 14) band model; dashed curve to Lawaetz (Ref. 17) band model; continuous curve to present band model.

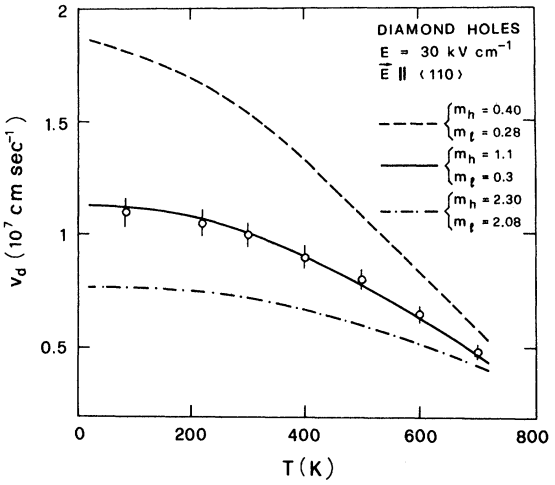

FIG. 7. Experimental (dots) and theoretical (lines) hole-drift velocity at fixed field strength as a function of temperature. Dot-dashed curve refers to Rauch (Ref. 14) band model, dashed curve to Lawaetz (Ref. 17) band model, continuous curve to present model.

treme cases for the values of the effective masses. As reported before from this figure it is seen that by scaling appropriately the value of the deformation potential parameters the temperature dependence of the mobility can be reproduced quantitatively within a comparable degree of accuracy in the temperature range considered. The discrepancy among different models, more evident below about 100 K, arises from the inclusion of acoustic dissipation which associates a higher mobility with the model with larger effective masses. However, the lack of experiments for temperatures below 85 K does not allow a detailed investigation on this effect to be carried out. It is worth noting that inclusion of acoustic dissipation and exact phonon population leads theoretical mobility to increase with decreasing temperatures more steeply than the rigorous $T^{-1.5}$ dependence usually cited, as reported by Gherardi *et al.*[36]

D. Drift velocity versus field

The reliability of the present model is checked by performing fitting of the drift velocity versus field curves in the whole temperature range considered. The results are illustrated in Fig. 3. There, theory and experiments have been found to agree within an uncertainty of about 20% which, in view of the approximations introduced in the model and of the experimental uncertainty, should be considered satisfactory.

Figure 7 reports data of the drift velocity at the highest field strength ($E = 30$ kV/cm) as a function of temperature. As discussed previously, in the saturated region the more enhanced sensitivity of the drift velocity to the effective mass as compared to other parameters is taken as a condition for the determination of the effective mass of heavy holes. The comparison of experiments with the results obtained with the different band models used for mobility (see Fig. 6) is illustrated in Fig. 7.

E. Mean-hole energy and repopulation

The mean energy of holes as calculated from Monte Carlo is reported at the indicated temperatures as a function of field strength in Fig. 8. The

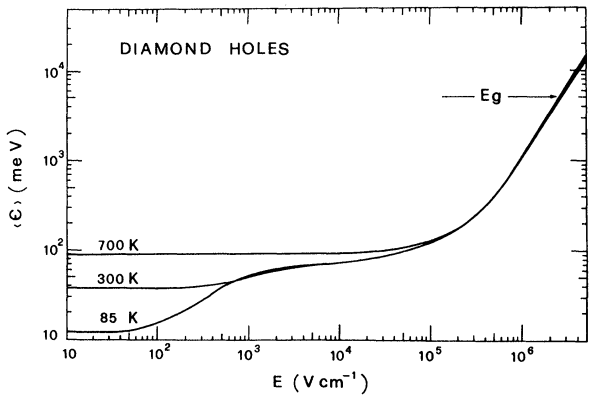

FIG. 8. Mean-hole energy as a function of electric field at the different temperatures indicated. E_g is the energy gap of diamond.

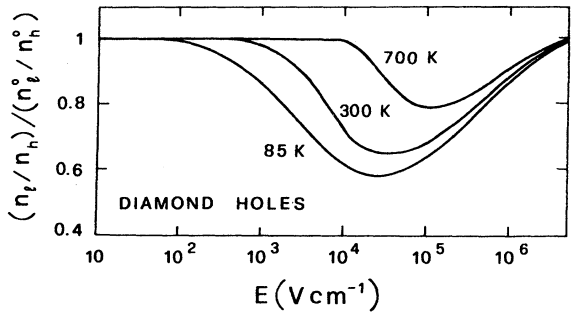

FIG. 9. Ratio of populations between light and heavy bands normalized to its equilibrium value n_l^0/n_h^0 as a function of field strength at the temperatures indicated.

value of the energy gap $E_g = 5.49$ eV reported in Fig. 8 should be taken as a reference point in the energy scale for distinguishing the realistic region of applicable field strengths. In this respect, it is worth noting that the mean energy crosses the energy gap value for fields above about 2×10^6 V/cm, in agreement with the experimental evidence of very high dielectric breakdown fields (up to 10^6 V/cm) for diamond.[21]

Figure 9 shows the field dependence of the ratio between light- and heavy-hole concentration normalized to its equilibrium value $(n_l/n_h)/(n_l^0/n_h^0)$. The decrease from the unit value at increasing field strength evidences a depopulation effect[29] arising from strong optical phonon scattering.

V. CONCLUSIONS

The hole-drift velocity in natural diamond is measured with the time-of-flight technique in a wide range of temperatures $85 \leq T \leq 700$ K and of field strengths $10^2 < E < 6\times10^4$ V/cm. The field is applied parallel to the ⟨110⟩ direction and at several temperatures, $85 \leq T \leq 300$ K, measurements are performed with the field applied parallel to the ⟨100⟩ direction also.

Drift mobility is reported for the first time in the temperature range $85 \leq T \leq 700$ K. Under nonlinear response conditions the drift velocity exhibits an anisotropic behavior with $v_{d\,100} \geq v_{d\,110}$. At the highest applied fields ($E \geq 25$ kV/cm) and for temperatures below about 300 K a saturation region of the drift velocity is found with a $v_s = 1.1 \pm 0.1\times10^7$ cm/sec.

The microscopic interpretation is carried out on the basis of a parabolic two-band model and uses a Monte Carlo technique. The fitting with experiments suggests values for the effective masses and deformation potential parameters for acoustic and nonpolar optical phonons. In particular, the values $m_h = 1.1m_0$, $m_l = 0.3m_0$ here found should be confirmed by a more careful determination of valence band parameters.

ACKNOWLEDGMENTS

The authors wish to thank Dr. S. Antoci, Dr. A. Baldereschi, and Dr. P. Lawaetz for having provided valuable information on the valence band structure of diamond. Dr. A. Matulis and Dr. C. Jacoboni are acknowledged for their suggestions and comments on many aspects of the subject. Dr. B. M. Vul, Dr. V. S. Vavilov, and Dr. E. A. Konorova are thanked for their interest and support. Computer facilities were kindly provided by the Modena University Computer Center, and x-ray diffraction analysis by MASPEC (CNR) laboratory. This work was partially supported by CNR (National Research Council, Italy).

[1] C. Canali, C. Jacoboni, F. Nava, G. Ottaviani, and A. Alberigi Quaranta, Phys. Rev. B 12, 2265 (1975).
[2] G. Ottaviani, L. Reggiani, C. Canali, F. Nava, and A. Alberigi Quaranta, Phys. Rev. B 12, 3318 (1975).
[3] L. Reggiani, C. Canali, F. Nava, and G. Ottaviani, Phys. Rev. B 16, 2781 (1977).
[4] C. Jacoboni, F. Nava, C. Canali, and G. Ottaviani, Phys. Rev. B (in press).
[5] Preliminary results on this subject have been reported in Refs. 6 and 7.
[6] C. Canali, C. Jacoboni, F. Nava, L. Reggiani, and S. F. Kozlov, in the *Proceedings of the International Conference on the Physics of Semiconductors*, edited by B. L. H. Wilson (The Institute of Physics, London, 1978), p. 327.
[7] L. Reggiani, S. Bosi, C. Canali, F. Nava, and S. F. Kozlov, Solid State Commun. 30, 333 (1979).
[8] V. S. Vavilov and E. A. Konorova, Usp. Fiz. Nauk 118, 611 (1976) [Sov. Phys. —Usp. 19, 301 (1976)].
[9] A. G. Redfield, Phys. Rev. 94, 526 (1954).
[10] I. G. Austin and R. Wolfe, Proc. Phys. Soc. London, Sect. B 69, 329 (1956).
[11] P. T. Wedepohl, Proc. Phys. Soc., London, Sect. B 70, 177 (1957).
[12] P. J. Dean, E. C. Lightowlers, and D. R. Wight, Phys. Rev. A 140, 352 (1965).
[13] E. A. Konorova and S. A. Schevchenko, Fiz. Tekh. Poluprovodn. 1, 364 (1967) [Sov. Phys.—Semicond. 1, 299 (1967)].
[14] C. J. Rauch, in *Proceedings of the 6th International Conference on the Physics of Semiconductors*, edited by A. C. Stickland (The Institute of Physics and the Physical Society, London, 1962), p. 276.
[15] P. E. Clegg and E. W. J. Mitchell, Proc. Phys. Soc., London 84, 31 (1964).
[16] G. G. Hall, Philos. Magazine 3, 429 (1958).

[17]P. Lawaetz, Phys. Rev. B 4, 3460 (1971); in this paper the γ_2 value of Table II should be corrected in $\gamma_2 = 0.42$; thus there is no sign difference between γ_2 and γ_3 and the formalism cited is valid (P. Lawaetz, private communication).
[18]G. Gagliani and L. Reggiani, Nuovo Cimento 30B, 207 (1975).
[19]A. Mainwood, J. Phys. C 12, 2543 (1979).
[20]S. F. Kozlov, R. Stuck, M. Hage-Ali, and P. Siffert, IEEE Trans. Nucl. Sci. 22, 160 (1975).
[21]C. De Blasi, S. Galassini, G. Micocci, L. Ruggiero, A. Tepore, F. Nava, C. Manfredotti, and S. F. Kozlov, Nucl. Instrum. Methods 163, 121 (1979).
[22]F. Nava, C. Canali, M. Artuso, E. Gatti, P. F. Manfredi, and S. F. Kozlov, IEEE Trans. Nucl. Sci. 26, 308 (1979).
[23]M. Martini, J. W. Mayer, and K. R. Zanio, in *Applied Solid State Science*, edited by R. Wolfe (Academic, New York, 1972), Vol. 3.
[24]A. Alberigi Quaranta, C. Canali, and G. Ottaviani, Rev. Sci. Instrum. 41, 1205 (1970).
[25]G. Ottaviani, C. Canali, C. Jacoboni, A. Alberigi Quaranta, and K. R. Zanio, J. Appl. Phys. 44, 360 (1973).
[26]C. Canali, M. Martini, G. Ottaviani, and K. R. Zanio, Phys. Rev. 4B, 422 (1971).
[27]H. Nakagawa and S. Zukotynski, Can. J. Phys. 56, 364 (1978).
[28]C. Jacoboni and L. Reggiani, Adv. Phys. 28, 493 (1979).
[29]S. Bosi, C. Jacoboni, and L. Reggiani, J. Phys. C 12, 1525 (1979).
[30]E. O. Kane, J. Phys. Chem. Solids 1, 82 (1956).
[31]M. Costato, G. Gagliani, C. Jacoboni, and L. Reggiani, J. Phys. Chem. Solids 35, 1605 (1974).
[32]W. Shockley, Bell Syst. Tech. J. 30, 990 (1951).
[33]J. L. Yarnell, J. L. Warren, and R. G. Wenzel, Phys. Rev. Lett. 13, 13 (1964).
[34]Handbook of Chemistry and Physics, edited by R. C. Weast (Chemical Rubber Co., Ohio, 1971).
[35]Derived from the values of the elastic constants reported by C. Kittel, *Introduction to Solid State Physics* (Wiley, New York, 1966).
[36]L. Gherardi, A. Pellacani, and C. Jacoboni, Lett. Nuovo Cimento 14, 225 (1975).